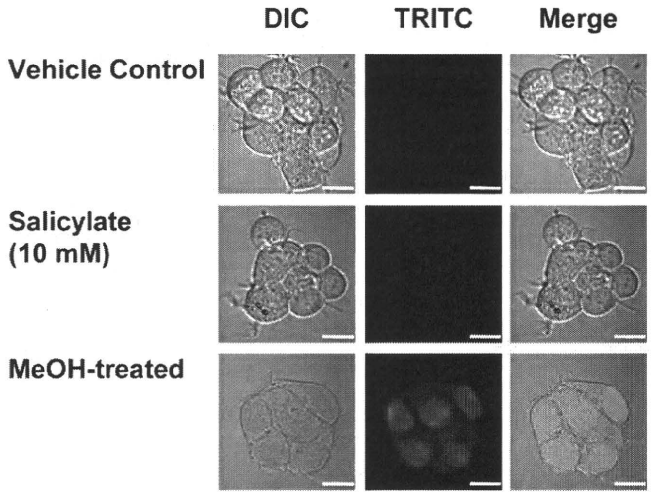

Fig. 4. Effects of salicylate on the viability of HEK293 cells. HEK293 cells were incubated for 12 h in medium containing 10% FBS in the presence or absence of 10 mM of salicylate. After incubation, the cells were stained with 7-AAD and observed by confocal microscopy. As a positive control, the membrane of cells incubated for 12 h in the absence of salicylate was permealyzed by methanol prior to the staining with 7-AAD. This figure indicates that 10 mM of salicylate has no cytotoxicity to HEK293 cells. The bar indicates 20 μm.

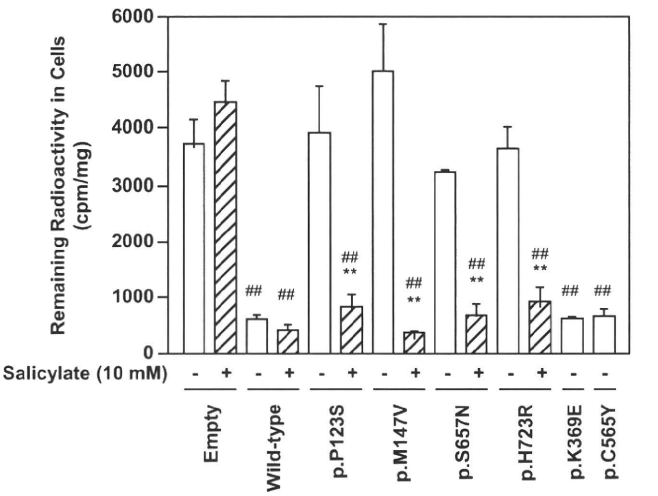

Fig. 6. Effects of salicylate on the iodide efflux from HEK293 cells. HEK293 cells were transfected with the empty vector, the expression vector including wild-type pendrin gene or the expression vector including the mutant genes. After 36 h, salicylate was added to the medium and the cells were further incubated for 12 h. The activity of pendrin was measured by radiolabeled-iodide efflux. The remaining radioactivity in cells was defined by dividing intracellular iodide content in the lysates (cpm/ml) by protein content in the lysates (mg/ml). This figure shows that the remaining radioactivity in the cells transfected with p.P123S, p.M147V, p.S657N and p.H723R was significantly decreased by salicylate. $^{**}P < 0.01$ vs. corresponding control (the cells lacking salicylate), $\#\#P < 0.01$ vs. empty without salicylate.

origin of electromotility of the outer hair cells (Zheng et al., 2000). The nonlinear capacitance change involved in prestin requires some ions such as Cl^- and $HCO3^-$ and is inhibited by 10 mM of salicylate (Oliver et al., 2001). Recently, we have reported that salicylate induces the translocation of prestin mutants to the plasma membrane from the cytoplasm (Kumano et al., 2010). There is approximately a 45% similarity between pendrin and prestin in amino acid sequences and transport of anions by pendrin is similar to those transported by prestin (Mount and Romero, 2004). Therefore, we hypothesized that as is the case with prestin, salicylate modifies the function as a pharmacological chaperone for the pendrin mutants. As shown in Figs. 3 and 6, salicylate induced the transport of 4 pendrin mutants, i.e., p.P123S, p.M147V, p.S657N and p.H723R, to the plasma membrane and the recovery of their anion exchanger activity, while 4 other pendrin mutants, i.e., p.A372V, p.N392Y, p.S666F and p.T721M, were retained in the cytoplasm.

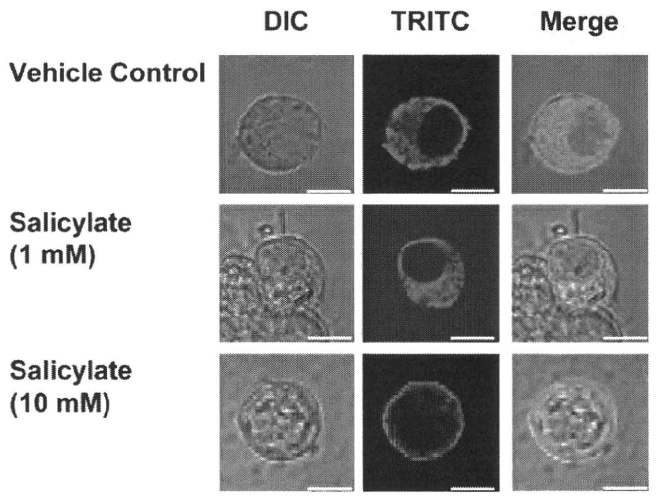

Fig. 5. Effects of lower concentration of salicylate on the intracellular localization of p.P123S mutant pendrin. HEK293 cells were transfected with the expression vector including p.P123S mutant pendrin. After 36 h, salicylate was added to the medium and the cells were further incubated for 12 h. Intracellular localization of pendrin was analyzed by immunofluorescent staining. This figure demonstrates that salicylate at 10 mM but not 1 mM induces the translocation of p.P123S mutant pendrin. The experiment shown is representative of 3 independent experiments. The bar indicates 10 μm.

Salicylate is a nonsteroidal anti-inflammatory drug (NSAID) which functions to inhibit cyclooxygenase-2 (COX-2) activity with an IC_{50} value of 14 μM (Cryer and Feldman, 1992; DuBois et al., 1996). Although salicylate at a concentration over 14 μM was expected to inhibit at least more than 50% of the COX-2 activity, in the present study, 1 mM salicylate did not induce the translocation of p.P123S pendrin mutants from the cytoplasm to the plasma membrane (Fig. 4). Therefore, it is unlikely that translocation of pendrin mutants to the plasma membrane by salicylate resulted from its COX2-inhibitory effect. Recently, it has been reported that salicylate also inhibits histone deacetylases (HDACs) at a concentration higher than that of COX-2 inhibition (DiRenzo et al., 2008). This might mean that inhibition of HDACs is one of the candidate mechanisms for the effect of salicylate on the translocation of pendrin mutants. Yoon et al. (2008) have reported that the p.H723R pendrin mutant is in the cytoplasm and is restored its location and $HCO3^-$ influx activity by 5 mM of sodium butyrate, which is an HDAC inhibitor (de Ruijter et al., 2003). HDACs are enzymes that remove the acetate from acetylated lysine residue in protein acetylated by histone acetyl transferases (HATs) (de Ruijter et al., 2003). Acetylation by HAT occurs in numerous proteins such as histone, transcription factors and heat shock proteins, and modifies their cellular functions (Ishihara et al., 2005). Therefore, hyperacetylated-proteins by the inhibition of HDACs induced by 10 mM of salicylate might lead to the translocation of pendrin mutants to the plasma membrane and recovery of their activity. In addition, it has been reported that glycosylation of pendrin effects its folding and ultimate localization (Yoon et al., 2008; Rebeh et al., 2009). Therefore, it is necessary to analyze the involvement of pendrin acetylation and glycosylation on the translocation and recovery of the activity of the pendrin mutants by 10 mM of salicylate.

In this study, we found that 4 mutants, i.e., p.P123S, p.M147V, p.S657N and p.H723R, were induced normal transport from the intracellular region and that they were restored their activity by

10 mM of salicylate, while 4 other mutants, i.e., p.A372V, p.N392Y, p.S666F and p.T721M, were not induced normal transport and were not restored their activity (Figs. 2 and 5). We confirmed that there was no significant difference in the protein levels of expression of wild-type pendrin and 10 pendrin mutants by Western blotting. Therefore, the recovery of the activity of 4 pendrin mutants, i.e., p.P123S, p.M147V, p.S657N and p.H723R, is considered to be due to the alterations in localization rather than to the level of protein expression. It has been reported that p.H723R pendrin mutant is mostly expressed in the endoplasmic reticulum, whereas p.L236P pendrin mutant is in the centrosomal region of the cells (Yoon et al., 2008). In that report, p.H723R but not p.L236P interestingly was restored its $HCO3^-$ influx activity by sodium butyrate. Therefore, it is possible that intracellular localization of pendrin mutants (p.P123S, p.M147V, p.S657N and p.H723R) targeted to the plasma membrane by salicylate differs from that of 4 other pendrin mutants (p.A372V, p.N392Y, p.S666F and p.T721M). Clarification of the mechanism by which salicylate induces the translocation of pendrin mutants is important and requires further study.

In this study, we showed that p.K369E and p.C565Y were expressed in the plasma membrane (Fig. 1) and acted to export iodide (Fig. 5), although pendrin genes with mutations in p.K369E and p.C565Y have been recognized as candidate genes in Japanese patients with NSEVA (Tsukamoto et al., 2003). It has been shown that p.S166N found in Korean patients was expressed in the plasma membrane with Cl^-/HCO_3^- exchange activity (Yoon et al., 2008). Recently, p.C565Y pendrin mutant has also been reported to be expressed on the plasma membrane, and the exchange activities for ions such as chloride and bicarbonate were reduced in comparison to wild-type pendrin but greater than the functional null control

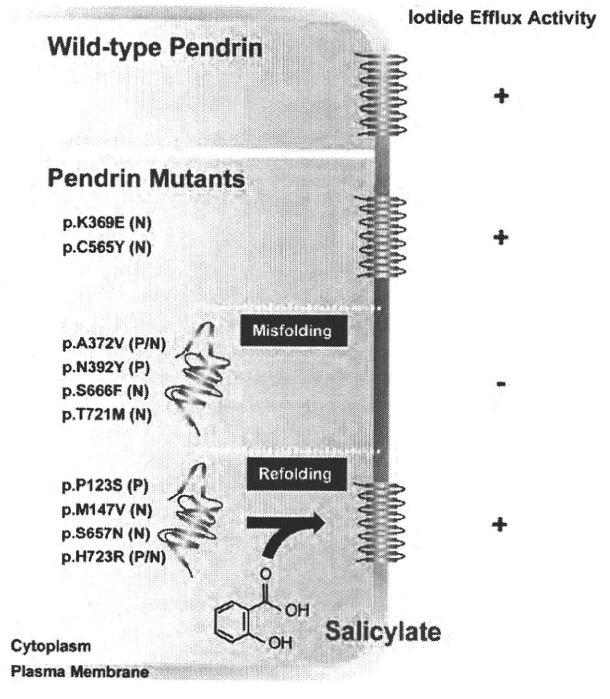

Fig. 7. Summary of pendrin mutants and *in vitro* effects of salicylate. Wild-type pendrin and two pendrin mutants, i.e., p.K369E and p.C565Y, are correctly folded, transported to the plasma membrane from the cytoplasm, and act to export iodide. In contrast, the other 8 pendrin mutants, i.e., p.P123S, p.M147V, p.A372V, p.N392Y, p.S657N, p.S666F, p.T721M and p.H723R, are retained in the cytoplasm. In the 8 pendrin mutants retained in the cytoplasm, 4 pendrin mutants, i.e., p.P123S, p.M147V, p.S657N and p.H723R, are translocated by salicylate to the plasma membrane, where the functions of 4 pendrin mutants are restored. The phenotypes (Pendred syndrome:P, NSEVA: N) related to the mutations reported by Tsukamoto et al. (2003) are represented.

(Choi et al., 2009). Thus, the relationship between those three mutations and NSEVA is unclear. As those three mutations were identified as compound heterozygous with other mutations in the pendrin gene (Tsukamoto et al., 2003; Park et al., 2004), it may be possible that NSEVA occurred when p.K369E, p.C565Y and p.S166N pendrin mutants were expressed with other pendrin mutants in the same cells. Further investigation is necessary to clarify how p.K369E and p.C565Y pendrin mutants are involved in NSEVA.

Pendred syndrome is characterized by sensorineural hearing impairment, presence of goiter, and a partial defect in iodide organification (Kopp et al., 2008). In the thyroid gland, pendrin releases iodide at the apical membrane of thyroid follicular cells into the follicular lumen to synthesize thyroid hormones, T3 and T4 (Kopp et al., 2008). Impairment of this function by pendrin mutants causes goiter and a partial defect in iodide organification. We have shown, in this study, that salicylate restores the iodide efflux activity of 4 pendrin mutants, i.e., p.P123S, p.M147V, p.S657N and p.H723R (Fig. 6), suggesting that salicylate restores the function in the thyroid. Although it is necessary to analyze the exchange activity for chloride and bicarbonate in the inner ear, salicylate could improve the condition of people suffering from Pendred syndrome caused by the mutation of p.P123S, p.M147V, p.S657N and p.H723R.

5. Conclusion

In conclusion, this is the report describing the intracellular localization of reported Japanese pendrin mutants. Of 10 pendrin mutants, 2 mutants and wild-type pendrin were found to be located in the plasma membrane, while 8 mutants were retained in the cytoplasm. Furthermore, we demonstrated that the function of 4 pendrin mutants was restored by salicylate (Fig. 7). This finding suggests that salicylate is a potentially promising compound for treatment of hearing loss that is associated with defects in protein localization, including a subset of individuals with Pendred syndrome. Our findings could contribute to further investigation for understanding disorders involving pendrin mutants.

Acknowledgements

This work was supported by Grant-in-Aid for Scientific Research on Priority Areas 15086202 from the Ministry of Education, Culture, Sports, Science and Technology of Japan, by Grant-in-Aid for Scientific Research (B) 20390439 from the Japan Society for the Promotion of Science, by Grant-in-Aid for Exploratory Research 20659263 from the Ministry of Education, Culture, Sports, Science and Technology of Japan, by a grant from the Human Frontier Science Program, by a Health and Labor Science Research Grant from the Ministry of Health, Labor and Welfare of Japan, by a grant from the Iketani Science and Technology Foundation, by a grant from the Daiwa Securities Health Foundation and by Tohoku University Global COE Program "Global Nano-Biomedical Engineering Education and Research Network Centre" to H.W.

References

Choi, B.Y., Stewart, A.K., Madeo, A.C., Pryor, S.P., Lenhard, S., Kittles, R., Eisenman, D., Kim, H.J., Niparko, J., Thomsen, J., Arnos, K.S., Nance, W.E., King, K.A., Zalewski, C.K., Brewer, C.C., Shawker, T., Reynolds, J.C., Butman, J.A., Karniski, L.P., Alper, S.L., Griffith, A.J., 2009. Hypo-functional SLC26A4 variants associated with nonsyndromic hearing loss and enlargement of the vestibular aqueduct: genotype–phenotype correlation or coincidental polymorphisms? Hum. Mutat. 30, 599–608.

Cryer, B., Feldman, M., 1992. Effects of nonsteroidal anti-inflammatory drugs on endogenous gastrointestinal prostaglandins and therapeutic strategies for prevention and treatment of nonsteroidal anti-inflammatory drug-induced damage. Arch. Intern. Med. 152, 1145–1155.

Conn, P.M., Leaños-Miranda, A., Janovick, J.A., 2002. Protein origami: therapeutic rescue of misfolded gene products. Mol. Interv. 2, 308–316.

de Ruijter, A.J., van Gennip, A.H., Caron, H.N., Kemp, S., van Kuilenburg, A.B., 2003. Histone deacetylases (HDACs): characterization of the classical HDAC family. Biochem. J. 370, 737–749.

DiRenzo, F., Cappelletti, G., Broccia, M.L., Giavini, E., Menegola, E., 2008. The inhibition of embryonic histone deacetylases as the possible mechanism accounting for axial skeletal malformations induced by sodium salicylate. Toxicol. Sci. 104, 397–404.

Dossena, S., Rodighiero, S., Vezzoli, V., Bazzini, C., Sironi, C., Meyer, G., Fürst, J., Ritter, M., Garavaglia, M.L., Fugazzola, L., Persani, L., Zorowka, P., Storelli, C., Beck-Peccoz, P., Bottá, G., Paulmichl, M., 2006. Fast fluorometric method for measuring pendrin (SLC26A4) Cl^-/I^- transport activity. Cell. Physiol. Biochem. 18, 67–74.

Dossena, S., Rodighiero, S., Vezzoli, V., Nofziger, C., Salvioni, E., Boccazzi, M., Grabmayer, E., Bottà, G., Meyer, G., Fugazzola, L., Beck-Peccoz, P., Paulmichl, M., 2009. Functional characterization of wild-type and mutated pendrin (SLC26A4), the anion transporter involved in Pendred syndrome. J. Mol. Endocrinol. 43, 93–103.

DuBois, R.N., Giardiello, F.M., Smalley, W.E., 1996. Nonsteroidal anti-inflammatory drugs, eicosanoids, and colorectal cancer prevention. Gastroenterol. Clin. North. Am. 25, 773–791.

Everett, L.A., Glaser, B., Beck, J.C., Idol, J.R., Buchs, A., Heyman, M., Adawi, F., Hazani, E., Nassir, E., Baxevanis, A.D., Sheffield, V.C., Green, E.D., 1997. Pendred syndrome is caused by mutations in a putative sulphate transporter gene (PDS). Nat. Genet. 17, 411–422.

Gillam, M.P., Sidhaye, A.R., Lee, E.J., Rutishauser, J., Stephan, C.W., Kopp, P., 2004. Functional characterization of pendrin in a polarized cell system. Evidence for pendrin-mediated apical iodide efflux. J. Biol. Chem. 279, 13004–13010.

Ishihara, K., Hong, J., Zee, O., Ohuchi, K., 2005. Mechanism of the eosinophilic differentiation of HL-60 clone 15 cells induced by n-butyrate. Int. Arch. Allergy Immunol. 137 (Suppl. 1), 77–82.

Janovick, J.A., Maya-Nunez, G., Conn, P.M., 2002. Rescue of hypogonadotropic hypogonadism-causing and manufactured GnRH receptor mutants by a specific protein-folding template: misrouted proteins as a novel disease etiology and therapeutic target. J. Clin. Endocrinol. Metab. 87, 3255–3262.

Kakehata, S., Santos-Sacchi, J., 1996. Effects of salicylate and lanthanides on outer hair cell motility and associated gating charge. J. Neurosci. 16, 4881–4889.

Kopp, P., 1999. Pendred's syndrome: clinical characteristics and molecular basis. Curr. Opin. Endocrinol. Diabetes 6, 261–269.

Kopp, P., Pesce, L., Solis-S, J.C., 2008. Pendred syndrome and iodide transport in the thyroid. Trends Endocrinol. Metab. 19, 260–268.

Kumano, S., Iida, K., Ishihara, K., Murakoshi, M., Tsumoto, K., Ikeda, K., Kumagai, I., Kobayashi, T., Wada, H., 2010. Salicylate-induced translocation of prestin having mutation in the GTSRH sequence to the plasma membrane. FEBS Lett. 584, 2327–2332.

Loo, T.W., Clarke, D.M., 1997. Correction of defective protein kinesis of human P-glycoprotein mutants by substrates and modulators. J. Biol. Chem. 272, 709–712.

Morello, J.P., Salahpour, A., Laperrière, A., Bernier, V., Arthus, M.F., Lonergan, M., Petäjä-Repo, U., Angers, S., Morin, D., Bichet, D.G., Bouvier, M., 2000. Pharmacological chaperones rescue cell-surface expression and function of misfolded V2 vasopressin receptor mutants. J. Clin. Invest. 105, 887–895.

Mount, D.B., Romero, M.F., 2004. SLC26 gene family of multifunctional anion exchangers. Pflugers Arch. 447, 710–721.

Oliver, D., He, D.Z., Klöcker, N., Ludwig, J., Schulte, U., Waldegger, S., Ruppersberg, J.P., Dallos, P., Fakler, B., 2001. Intracellular anions as the voltage sensor of prestin, the outer hair cell motor protein. Science 292, 2340–2343.

Park, H.J., Lee, S.J., Jin, H.S., Lee, J.O., Go, S.H., Jang, H.S., Moon, S.K., Lee, S.C., Chun, Y.M., Lee, H.K., Choi, J.Y., Jung, S.C., Griffith, A.J., Koo, S.K., 2004. Genetic basis of hearing loss associated with enlarged vestibular aqueducts in Koreans. Clin. Genet. 67, 160–165.

Rebeh, I.B., Yoshimi, N., Hadj-Kacem, H., Yanohco, S., Hammami, B., Mnif, M., Araki, M., Ghorbel, A., Ayadi, H., Masmoudi, S., Miyazaki, H., 2009. Two missense mutations in SLC26A4 gene: a molecular and functional study. Clin. Genet. 78, 74–80.

Rotman-Pikielny, P., Hirschberg, K., Maruvada, P., Suzuki, K., Royaux, I.E., Green, E.D., Kohn, L.D., Lippincott-Schwartz, J., Yen, P.M., 2002. Retention of pendrin in the endoplasmic reticulum is a major mechanism for Pendred syndrome. Hum. Mol. Genet. 11, 2625–2633.

Royaux, I.E., Wall, S.M., Karniski, L.P., Everett, L.A., Suzuki, K., Knepper, M.A., Green, E.D., 2001. Pendrin, encoded by the Pendred syndrome gene, resides in the apical region of renal intercalated cells and mediates bicarbonate secretion. Proc. Natl. Acad. Sci. USA 98, 4221–4226.

Scott, D.A., Wang, R., Kreman, T.M., Sheffield, V.C., Karniski, L.P., 1999. The Pendred syndrome gene encodes a chloride–iodide transport protein. Nat. Genet. 21, 440–443.

Taubes, G., 1996. Misfolding the way to disease. Science 271, 1493–1495.

Thomas, P.J., Qu, B.H., Pedersen, P.L., 1995. Defective protein folding as a basis of human disease. Trends Biochem. Sci. 20, 456–459.

Tsukamoto, K., Suzuki, H., Harada, D., Namba, A., Abe, S., Usami, S., 2003. Distribution and frequencies of PDS (SLC26A4) mutations in Pendred syndrome and nonsyndromic hearing loss associated with enlarged vestibular aqueduct: a unique spectrum of mutations in Japanese. Eur. J. Hum. Genet. 11, 916–922.

Tunstall, M.J., Gale, J.E., Ashmore, J.F., 1995. Action of salicylate on membrane capacitance of outer hair cells from the guinea-pig cochlea. J. Physiol. 485, 739–752.

Ulloa-Aguirre, A., Janovick, J.A., Brothers, S.P., Conn, P.M., 2004. Pharmacologic rescue of conformationally-defective proteins: implications for the treatment of human disease. Traffic 5, 821–837.

Wangemann, P., Nakaya, K., Wu, T., Maganti, R.J., Itza, E.M., Sanneman, J.D., Harbidge, D.G., Billings, S., Marcus, D.C., 2007. Loss of cochlear $HCO3^-$ secretion causes deafness via endolymphatic acidification and inhibition of Ca^{2+} reabsorption in a Pendred syndrome mouse model. Am. J. Physiol. Renal Physiol. 292, F1345–F1353.

Welch, W.J., Brown, C.R., 1996. Influence of molecular and chemical chaperones on protein folding. Cell Stress Chaperones 1, 109–115.

Yoon, J.S., Park, H.J., Yoo, S.Y., Namkung, W., Jo, M.J., Koo, S.K., Park, H.Y., Lee, W.S., Kim, K.H., Lee, M.G., 2008. Heterogeneity in the processing defect of SLC26A4 mutants. J. Med. Genet. 45, 411–419.

Yoshino, T., Sato, E., Nakashima, T., Nagashima, W., Teranishi, M.A., Nakayama, A., Mori, N., Murakami, H., Funahashi, H., Imai, T., 2004. The immunohistochemical analysis of pendrin in the mouse inner ear. Hear. Res. 195, 9–16.

Zheng, J., Shen, W., He, D.Z., Long, K.B., Madison, L.D., Dallos, P., 2000. Prestin is the motor protein of cochlear outer hair cells. Nature 405, 149–155.

FEBS Letters 584 (2010) 2872–2876

ELSEVIER

FEBS Letters

journal homepage: www.FEBSLetters.org

Atomic force microscopy imaging of the structure of the motor protein prestin reconstituted into an artificial lipid bilayer

Shun Kumano, Michio Murakoshi, Koji Iida, Hiroshi Hamana, Hiroshi Wada *

Department of Bioengineering and Robotics, Tohoku University, 6-6-01 Aoba-yama, Sendai 980-8579, Japan

ARTICLE INFO

Article history:
Received 2 March 2010
Revised 29 April 2010
Accepted 30 April 2010
Available online 7 May 2010

Edited by Sandro Sonnino

Keywords:
Prestin
Membrane protein
Atomic force microscopy
Outer hair cell
Inner ear

ABSTRACT

Prestin is the motor protein of cochlear outer hair cells and is essential for mammalian hearing. The present study aimed to clarify the structure of prestin by atomic force microscopy (AFM). Prestin was purified from Chinese hamster ovary cells which had been modified to stably express prestin, and then reconstituted into an artificial lipid bilayer. Immunofluorescence staining with anti-prestin antibody showed that the cytoplasmic side of prestin was possibly face up in the reconstituted lipid bilayer. AFM observation indicated that the cytoplasmic surface of prestin was ring-like with a diameter of about 11 nm.

1. Introduction

The basis of electromotility of outer hair cells (OHCs) which realizes the high sensitivity of mammalian hearing is considered to be the motor protein prestin [1]. Several characteristics of prestin have been gradually clarified [2]. Murakoshi et al. [3] detected prestin in the plasma membrane of prestin-transfected Chinese hamster ovary (CHO) cells using Qdots as topographic markers and observed ring-like structures, possibly prestin, by atomic force microscopy (AFM). Mio et al. [4] observed prestin purified from prestin-transfected insect cells by transmission electron microscopy (TEM) and found prestin to be a bullet-shaped molecule. Although those two studies are significant, their observed images differed, indicating that the structure of prestin was unclear. Thus, the aim of the present study was to clarify such structure by reconstitution of purified prestin into an artificial lipid bilayer and observation of the prestin-reconstituted lipid bilayer by AFM.

2. Materials and methods

2.1. Purification of prestin

The purification of prestin was performed by the method established in our previous study with some modifications [5]. CHO cells which had been modified to stably express C-terminal 3×FLAG-tagged prestin were suspended in Tris–KCl buffer (10 mM Tris, 150 mM KCl, pH 7.4) and sonicated, followed by centrifugation at 1000×*g* for 7 min at 4 °C to remove nuclei and undisrupted cells. The obtained supernatant was centrifuged at 20360×*g* at 4 °C for 2 h to collect the membrane fraction of the cells. Membrane proteins were solubilized by resuspending the obtained membrane fraction in Tris–KCl buffer containing 10 mM *n*-nonyl-β-D-thiomaltopyranoside (NTM, Dojindo, Kumamoto, Japan). After 3-h incubation on ice, samples were centrifuged at 20360×*g* at 4 °C for 3 h to remove non-solubilized proteins. The supernatant was applied to a column filled with anti-FLAG affinity gel (Sigma–Aldrich, St. Louis, MO). The column was then washed with Tris–KCl buffer containing 0.065 mM Fos-Cholin-16 (Anatrace, Maumee, OH) to replace the detergent NTM with Fos-Choline-16. Afterward, prestin was competitively eluted with 1 ml of that buffer containing 500 μg/ml of 3×FLAG peptide (Sigma–Aldrich). Whether prestin was purified or not was confirmed by SDS–PAGE, followed by Western blotting with anti-FLAG antibody and HRP-conjugated anti-mouse IgG antibody and by silver staining.

Abbreviations: OHC, outer hair cell; CHO, Chinese hamster ovary; AFM, atomic force microscopy; TEM, transmission electron microscopy

* Corresponding author. Hiroshi Wada, Department of Bioengineering and Robotics, Tohoku University, 6-6-01 Aoba-yama, Sendai 980-8579, Japan. Fax: +81 22 795 6939.
E-mail address: wada@cc.mech.tohoku.ac.jp (H. Wada).

0014-5793/$36.00
doi:10.1016/j.febslet.2010.04.076

2.2. Reconstitution of prestin into a preformed lipid bilayer

The method of direct reconstitution of membrane proteins into a preformed lipid bilayer was applied in the present study [6]. An artificial lipid bilayer was formed on mica using dioeoyl-phosphatidylcholine (DOPC) and dipalmitoyl-phosphatidylcholine (DPPC) (Avanti Polar Lipids, Alabaster, AL). The lipid bilayer was preincubated for 30 min at 4 °C with Tris–KCl buffer containing 5 mM $CaCl_2$ and 0.0065 mM Fos-cholin-16 for equilibration of the detergent within the lipid bilayer. Afterward, such bilayer was incubated with Tris–KCl buffer containing purified prestin, 5 mM $CaCl_2$ and 0.039 mM Fos-cholin-16 for 15 min at 4 °C. Excess prestin was then removed by extensive rinsing with Tris–KCl buffer. As a negative control, the lipid bilayer treated with detergent but without prestin was also prepared.

2.3. Staining of prestin in the reconstituted lipid bilayer

The existence of prestin in the lipid bilayer was confirmed by immunofluorescence staining. The prestin-reconstituted lipid bilayer was incubated with Block Ace (Dainippon Pharmaceutical Co. Osaka, Japan) for 30 min at 37 °C to avoid non-specific binding of antibodies. Afterward, that bilayer was stained with goat anti-prestin N-terminus primary antibody (Santa Cruz Biotechnology, Santa Cruz, CA, USA) at a dilution of 1:100 in PBS overnight at 4 °C and with anti-goat IgG Texas Red (Santa Cruz Biotechnology) at a dilution of 1:200 in PBS at 37 °C for 60 min. The stained lipid bilayer was observed by confocal microscopy.

2.4. AFM imaging

The height images of the lipid bilayer were acquired in Tris–KCl buffer filtered with a 0.2-μm nylon filter by Multimode V AFM with a Nanoscope V controller (Veeco, Santa Barbara, CA) at 24–26 °C. V-shaped Si_3N_4 cantilevers (OMCL-TR400PSA-2, Olympus, Tokyo, Japan) with a spring constant of 0.06 N/m were used. The AFM was operated in the oscillation imaging mode (Tapping mode™, Digital Instruments) at a scan frequency of 1–0.5 kHz. In the present study, three types of images were obtained by AFM, namely, low- (5.0 × 5.0 μm), middle- (1.0 × 1.0 μm) and high-magnification images (300 × 300 nm). Each scan line has 256 and 512 points of data and an image consists of 256 and 512 scan lines for low magnification images and for middle- and high-magnification images, respectively. Obtained AFM images were flattened by use of a software program (NanoScope v7.00, Veeco) to eliminate background slopes and to correct dispersions of individual scanning lines. In addition, only high-magnification images were low-pass filtered to reduce high frequency noise. When the observed structure was ring-like, the distance between two peaks based on the cross sections was taken to be its diameter, as was done in our previous study [3].

3. Results

3.1. Purification of prestin

Whether prestin was indeed purified or not was investigated by SDS–PAGE, followed by Western blotting and silver staining. Results of Western blotting and silver staining are shown in Fig. 1A and B, respectively. In the Western blotting image, the 100 kDa band, probably showing prestin, was detected. In the results of silver staining, only one band corresponding to the band observed in Western blotting was recognized.

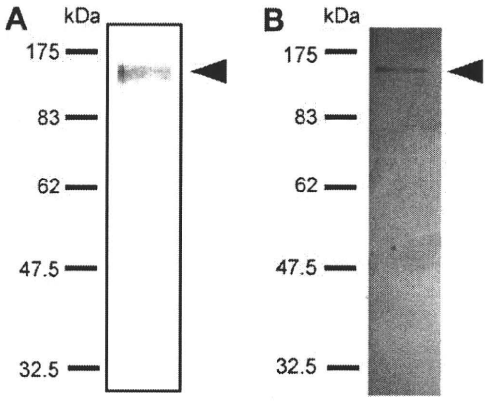

Fig. 1. Results of Western blotting and silver staining. (A) Western blotting data. A 100 kDa band probably showing prestin is seen. (B) Result of silver staining of SDS–PAGE gel. Only one band at 100 kDa, which was thought to correspond to the band detected in the result of Western blotting, is recognized.

3.2. Immunofluorescence staining of the prestin-reconstituted lipid bilayer

After the reconstitution process, immunofluorescence staining was employed to investigate whether prestin had been incorporated into the preformed lipid bilayer. Representative immunofluorescence images of the prestin-reconstituted lipid bilayer and negative control sample are shown in Fig. 2. Red fluorescence was detected in the prestin-reconstituted lipid bilayer but not in the negative control sample.

3.3. AFM imaging of the lipid bilayer

The AFM height image of the lipid bilayer without treatment showed two kinds of flat domains (Fig. 3A). A similar image was also obtained from the negative control sample (Fig. 3B). Unlike those two images, in addition to the flat domain, bumpy domains indicated by white arrows were detected in the low magnification AFM image of the prestin-reconstituted lipid bilayer (Fig. 3C). The boxed area in Fig. 3C was scanned by AFM and the obtained image is depicted in Fig. 3D. Dense small particles, some of which were recognized as ring-like structures, can be observed in that image. To clearly visualize the observed particles, the boxed area in Fig. 3D was scanned by AFM, the acquired image being shown in Fig. 3E. Moreover, three-dimensional representation of Fig. 3E is depicted in Fig. 4. Many ring-like structures were confirmed to be densely embedded in the lipid bilayer. The average diameter of such structures in Fig. 3E and other AFM images which are not shown here is 11.0 ± 1.3 nm (n = 42).

4. Discussion

4.1. Reconstitution of prestin into an artificial lipid bilayer

After the purification process, only the 100 kDa band corresponding to the band in Western blotting data was detected by silver staining of SDS–PAGE gel, indicating that prestin had been purified. The 100 kDa band probably shows the monomer of prestin. As SDS possibly affects the binding between prestin molecules, to clearly confirm the oligomerization of purified prestin, a mild detergent such as perfluoro-octanoic acid should be used as in the study by Zheng et al. [7]. The AFM height image of the lipid bilayer without treatment shows two types of flat domains (Fig. 3A), as seen in previous studies [6,8–11]. At 24–26 °C, DOPC forms fluid-phase domains, while DPPC forms gel-phase domains. The thickness of DPPC in the gel-phase is larger than that of DOPC in

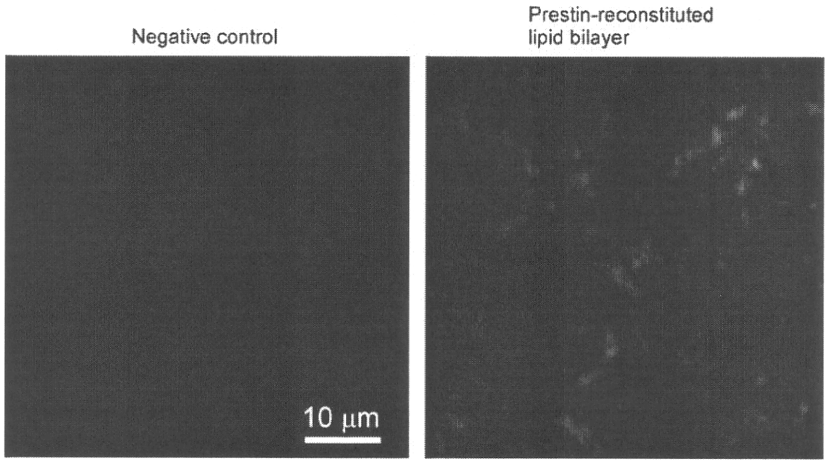

Fig. 2. Immunofluorescence staining of prestin-reconstituted lipid bilayer. Negative control sample and the prestin-reconstituted lipid bilayer were stained with anti-prestin antibody and anti-goat IgG Texas Red. Red fluorescence indicating the existence of prestin is only found in the prestin-reconstituted lipid bilayer.

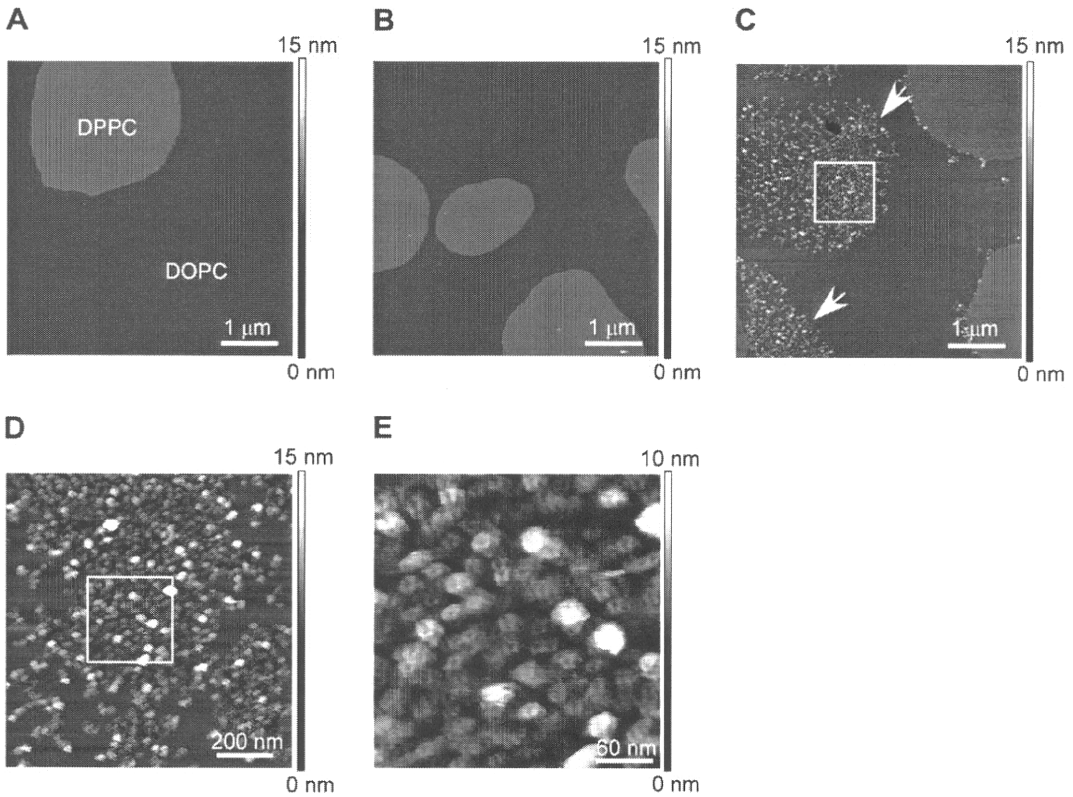

Fig. 3. AFM height images of the lipid bilayer. (A) AFM image of the lipid bilayer without treatment at low magnification. (B) AFM image of the negative control sample at low magnification. (C) AFM image of prestin-reconstituted lipid bilayer at low magnification. (D) Middle-magnification image obtained by scanning of the boxed area shown in (C). (E) High-magnification image obtained by scanning of the boxed area shown in (D). Two kinds of flat domains in (A) and (B) probably represent the domain of DPPC in the gel-phase and that of DOPC in the fluid-phase. Bumpy domains indicated by white arrows can be detected in the prestin-reconstituted lipid bilayer shown in (C). Many small particles can be found in the middle-magnification AFM images and those particles were recognized as ring-like in the high-magnification image. Such ring-like structures probably show prestin molecules.

the fluid-phase, thus indicating that the two types of observed domains were due to the difference in the thickness between the two lipids. After the reconstitution process, immunofluorescence staining using anti-prestin antibody showed that prestin existed in the reconstituted lipid bilayer (Fig. 2). In the AFM image, the bumpy domains, which probably corresponded to prestin, were recognized only in DOPC domains of the prestin-reconstituted lipid bilayer. Milhiet et al. [6] have also suggested that proteins of interest were reconstituted only into the DOPC domains in the fluid state. Thus, the present study and their study imply that proteins tend to be reconstituted into the DOPC domains in the fluid state. In the AFM image at high-magnification, ring-like structures probably showing prestin were densely reconstituted into the lipid bilayer. However, the alignment of such structures as found in the OHC plasma membrane by Sinha et al. [12] was not detected, which might have resulted from differences in the environment

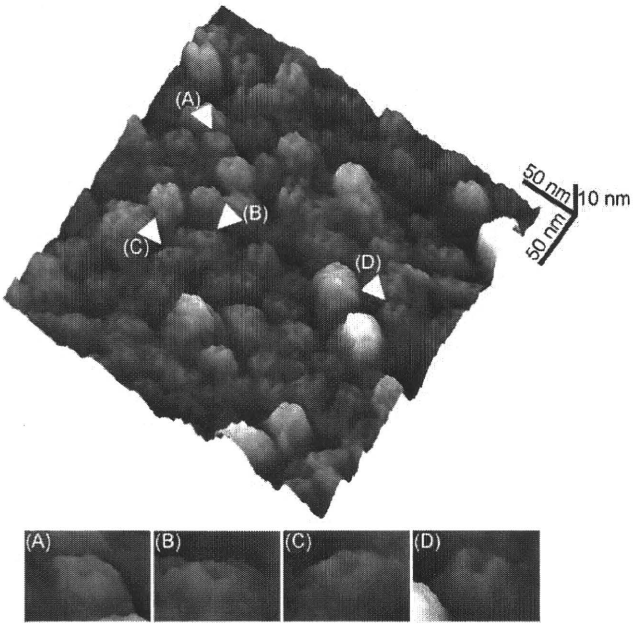

Fig. 4. Three-dimensional AFM height image of the prestin-reconstituted lipid bilayer. This figure was created from Fig. 3E. Representative examples of ring-like structures were digitally magnified and are shown (A and B). Ring-like structures, considered to be similar to those observed in the study of Murakoshi et al. [3], are found to be densely embedded in the lipid bilayer.

Table 1
Comparison of the size of prestin.

Sample	Method	Diameter (nm)	References
OHC plasma membrane	AFM	11–25	Le Grimellec et al. [15]
Purified prestin	TEM	7.7–9.6	Mio et al. [4]
Prestin-expressing CHO cell plasma membrane	AFM	9.6/13.0	Murakoshi et al. [3]
OHC plasma membrane	AFM	10	Sinha et al. [12]
Prestin-reconstituted lipid bilayer	AFM	11.0 ± 1.3	This study

between the OHC plasma membrane and the artificial lipid bilayer. The existence of actin cytoskeleton in OHCs and that of mica in the present study would affect the alignment of prestin.

4.2. Orientation of prestin

The orientation of prestin should be considered to confirm which side of prestin was observed by AFM, the extracellular side or the cytoplasmic side. Previous reports have suggested that when membrane proteins were reconstituted into a preformed lipid bilayer as done in the present study, their unidirectional orientation was obtained [6,13,14], indicating that all prestin molecules reconstituted into the lipid bilayer might be oriented in the same direction. In the present study, the standard deviation of the diameter of the observed ring-like structure, 1.3 nm, was small. Small standard deviation might increase the possibility that only either prestin molecules whose extracellular side was exposed or such molecules whose cytoplasmic side was exposed existed in the reconstituted lipid bilayer. Data showed in the previous reports, small standard deviation of the diameter and successful staining of such bilayer with anti-prestin antibody which binds to the cytoplasmic side of prestin possibly implied that the cytoplasmic side of prestin was face up. Although the possibility that the extracellular side of a few prestin molecules was exposed was not completely ruled out, it was considered that AFM possibly visualized the cytoplasmic side of prestin in the present study.

4.3. Structure and size of prestin

The AFM image of the prestin-reconstituted lipid bilayer showed dense ring-like structures, each with a diameter of 11.0 ± 1.3 nm, which were probably the surface structure of the cytoplasmic side of prestin. The previously reported sizes of prestin obtained by observation of the cytoplasmic side of prestin are listed in Table 1 [3,4,12,15]. Although it is unclear whether the particles detected in OHC plasma membranes are only comprised of prestin or not, our result is consistent with the previously reported sizes, supporting the assumption that the observed structures were prestin.

Le Grimellec et al. [15] found structures with a central depression in the cytoplasmic side of the OHC plasma membrane by AFM. Murakoshi et al. [3] showed by AFM that prestin might form a ring-like structure. On the other hand, Mio et al. [4] suggested that prestin is a bullet-shaped molecule which protrudes into the cytoplasmic side. Although Sinha et al. [12] found 10-nm particles in the cytoplasmic side of the OHC plasma membrane by AFM, whether those particles were ring-like or not was not specified. Thus, the structure of prestin has been a controversial issue. Our results demonstrate that prestin may form a ring-like structure with a diameter of about 11 nm, which agrees with results of Le Grimellec et al. [15] and Murakoshi et al. [3].

In summary, the present study attempted to visualize prestin purified and reconstituted into the artificial lipid bilayer by AFM. From the obtained AFM image, the cytoplasmic surface of prestin was indicated to be ring-like with a diameter of about 11 nm.

Acknowledgements

This work was supported by Grant-in-Aid for Scientific Research on Priority Areas 15086202 from the Ministry of Education, Culture, Sports, Science and Technology of Japan, by Grant-in-Aid for Scientific Research (B) 18390455 from the Japan Society for the Promotion of Science, by Grant-in-Aid for Exploratory Research 18659495 from the Ministry of Education, Culture, Sports, Science and Technology of Japan, by a grant from the Human Frontier Science Program, by a Health and Labour Science Research Grant from the Ministry of Health, Labour and Welfare of Japan, and by Tohoku University Global COE Program "Global Nano-Biomedical Engineering Education and Research Network Centre" to H.W., and by a Grant-in-Aid for JSPS Fellows from the Japan Society for the Promotion of Science to S.K.

References

[1] Zheng, J., Shen, W., He, D.Z.Z., Long, K.B., Madison, L.D. and Dallos, P. (2000) Prestin is the motor protein of cochlear outer hair cells. Nature 405, 149–155.
[2] Ashmore, J. (2008) Cochlear outer hair cell. Physiol. Rev. 88, 173–210.
[3] Murakoshi, M., Iida, K., Kumano, S. and Wada, H. (2009) Immune atomic force microscopy of prestin-transfected CHO cells using quantum dots. Pflugers Arch. 457, 885–898.
[4] Mio, K., Kubo, Y., Ogura, T., Yamamoto, T., Arisaka, F. and Sato, C. (2008) The motor protein prestin is a bullet-shaped molecule with inner cavities. J. Biol. Chem. 283, 1137–1145.
[5] Iida, K., Murakoshi, M., Kumano, S., Tsumoto, K., Ikeda, K., Kobayashi, T., Kumagai, I. and Wada, H. (2008) Purification of the motor protein prestin from Chinese hamster ovary cells stably expressing prestin. JBSE 3, 221–234.
[6] Milhiet, P.E., Gubellini, F., Berquand, A., Dosset, P., Rigaud, J.L., Le Grimellec, C. and Levy, D. (2006) High-resolution AFM of membrane proteins directly incorporated at high density in planar lipid bilayer. Biophys. J. 91, 3268–3275.
[7] Zheng, J., Du, G.G., Anderson, C.T., Keller, J.P., Orem, A., Dallos, P. and Cheatham, M. (2006) Analysis of the oligomeric structure of the motorprotein prestin. J. Biol. Chem. 281, 19916–19924.
[8] Morandat, S. and Kirat, K.E. (2006) Membrane resistance to Triton X-100 explored by real-time atomic force microscopy. Langmuir 22, 5786–5791.

[9] Berquand, A., Levy, D., Gubellini, F., Le Grimellec, C. and Milhiet, P. (2007) Influence of calcium on direct incorporation of membrane proteins into in-plane lipid bilayer. Ultramicroscopy 107, 928–933.
[10] Francius, G., Dufour, S., Deleu, M., Paquot, M., Mingeot-Leclercq, M. and Dufrêne, Y.E. (2008) Nanoscale membrane activity of surfactins: influence of geometry, charge and hydrophobicity. Biochim. Biophys. Acta 1778, 2058–2068.
[11] Mingeot-Leclercq, M., Deleu, M., Brasseur, R. and Dufrêne, Y.F. (2008) Atomic force microscopy of supported lipid bilayers. Nat. Protoc. 3, 1654–1659.
[12] Sinha, G.P., Sabri, F., Dimitriadis, E.K. and Iwasa, K.H. (2010) Organization of membrane motor in outer hair cells: an atomic force microscopic study. Pflugers Arch. 459, 427–439.
[13] Rigaud, J., Paternostre, M. and Bluzat, A. (1988) Mechanism of membrane protein insertion into liposomes during reconstitution procedures involving the use of detergents. 2. Incorporation of the light-driven proton pump bacteriorhodopsin. Biochemistry 27, 2677–2688.
[14] Rigaud, J., Pitard, B. and Levy, D. (1995) Reconstitution of membrane proteins into liposome: application to energy-transducing membrane proteins. Biochim. Biophys. Acta 1231, 223–246.
[15] Le Grimellec, C., Giocondi, M.C., Lenoir, M., Vater, M., Sposito, G. and Pujol, R. (2002) High-resolution three-dimensional imaging of the lateral plasma membrane of cochlear outer hair cells by atomic force microscopy. J. Comp. Neurol. 451, 62–69.

FEBS Letters 584 (2010) 2327–2332

ELSEVIER

FEBS Letters

journal homepage: www.FEBSLetters.org

Salicylate-induced translocation of prestin having mutation in the GTSRH sequence to the plasma membrane

Shun Kumano [a], Koji Iida [a], Kenji Ishihara [a], Michio Murakoshi [a], Kouhei Tsumoto [b], Katsuhisa Ikeda [c], Izumi Kumagai [d], Toshimitsu Kobayashi [e], Hiroshi Wada [a,*]

[a] Department of Bioengineering and Robotics, Tohoku University, Sendai, Japan
[b] Department of Medical Genome Sciences, The University of Tokyo, Kashiwa, Japan
[c] Department of Otorhinolaryngology, Juntendo University School of Medicine, Tokyo, Japan
[d] Department of Biomolecular Engineering, Tohoku University, Sendai, Japan
[e] Department of Otolaryngology, Head and Neck Surgery, Tohoku University Graduate School of Medicine, Sendai, Japan

ARTICLE INFO

Article history:
Received 14 February 2010
Revised 24 March 2010
Accepted 7 April 2010
Available online 11 April 2010

Edited by Gianni Cesareni

Keywords:
Prestin
Motor protein
Mutation
Salicylate
Outer hair cell
Inner ear

ABSTRACT

Prestin is a key molecule for mammalian hearing. The present study investigated changes in characteristics of prestin by culturing prestin-transfected cells with salicylate, an antagonist of prestin. As a result, the plasma membrane localization of prestin bearing a mutation in the GTSRH sequence, which normally accumulates in the cytoplasm, was recovered. Moreover, the nonlinear capacitance of the majority of the mutants, which is a signature of prestin activity, was also recovered. Thus, the present study discovered a new effect of salicylate on prestin, namely, the promotion of the plasma membrane expression of prestin mutants in an active state.

1. Introduction

The motor protein prestin in the plasma membrane of cochlear outer hair cells (OHCs) is believed to be the origin of their electromotility [1]. So far, several characteristics of prestin have been clarified by introduction of mutations into prestin [2]. Mutations in membrane proteins sometimes cause the accumulation of these proteins in the cytoplasm. It has been reported that when the cells expressing such accumulated mutants were cultured with a pharmacological chaperone, which is a cell membrane-permeable molecule with high affinity for these mutants, the chaperone bound to them and promoted their transport to the plasma membrane in an active state [3–7]. Salicylate, which is known as an antagonist of prestin, is thought to have cell membrane permeability with high affinity for prestin [8,9]. Thus, salicylate was considered to be a candidate molecule to work as a pharmacological chaperone for prestin. In the present study, the aim was to investigate whether or not salicylate has the ability to promote the plasma membrane expression of prestin mutants accumulated in the cytoplasm.

2. Materials and methods

2.1. Prestin mutants

Our previous study showed that mutations in the GTSRH sequence at positions 127–131 of prestin caused a decrease in nonlinear capacitance (NLC), which is a signature of prestin activity [10]. Such decrease may be due to the accumulation of prestin in the cytoplasm. Thus, the present study used the prestin mutants created in our previous study, namely, G127A, T128A, S129A, R130A, H131A and S129T. These mutants were engineered to be expressed in HEK293 cells by transfection. As the prestin genes were co-transfected with green fluorescent protein (GFP) gene into the cells, transfected cells were selected by GFP observation.

Abbreviations: OHC, outer hair cell; NLC, nonlinear capacitance; GFP, green fluorescent protein; WT, wild-type; WGA, wheat germ agglutinin

* Corresponding author at: Address: Department of Bioengineering and Robotics, Tohoku University, 6-6-01 Aoba-yama, Sendai 980-8579, Japan. Fax: +81 22 795 6939.
E-mail address: wada@cc.mech.tohoku.ac.jp (H. Wada).

0014-5793/$36.00 © 2010 Federation of European Biochemical Societies. Published by Elsevier B.V. All rights reserved.
doi:10.1016/j.febslet.2010.04.010

2.2. Incubation of transfected cells with salicylate

Transfected cells were cultured with salicylate, which is generally known to have the ability to suppress NLC as an antagonist of prestin, to confirm another effect of salicylate as a pharmacological chaperon for prestin. It was reported that, in the patch-clamp recording, 10 mM salicylate around the cells was required for almost complete suppression of NLC, which might be realized by the binding of salicylate with prestin in the plasma membrane [9]. Thus, for the binding of salicylate with prestin, at least 10 mM salicylate was considered to be necessary. Although salicylate possibly affects the cell viability, it has been reported that more than 85% of HEK293 cells were able to survive in the presence of up to 10 mM sodium salicylate [11]. In the present study, the cells were cultured for 24-36 hours in growth medium with sodium salicylate at a concentration of 10 mM from 12 hours after transfection. After such incubation, the cells were used in experiments. The cells cultured without salicylate were employed as control samples. Samples of the cells expressing wild-type (WT) prestin and its mutants which were cultured with 10 mM salicylate were termed WT prestin+Sal, G127A+Sal, T128A+Sal, S129A+Sal, R130A+Sal, H131A+Sal and S129T+Sal.

2.3. Confirmation of the localization of prestin in transfected cells

The localization of prestin in the cells was assessed by immunofluorescence staining with anti-FLAG antibody, TRITC-conjugated anti-mouse IgG antibody and wheat germ agglutinin (WGA)-Alexa Fluor 633 conjugate as described in our previous study [12]. In the present study, several tens of transfected cells were observed for

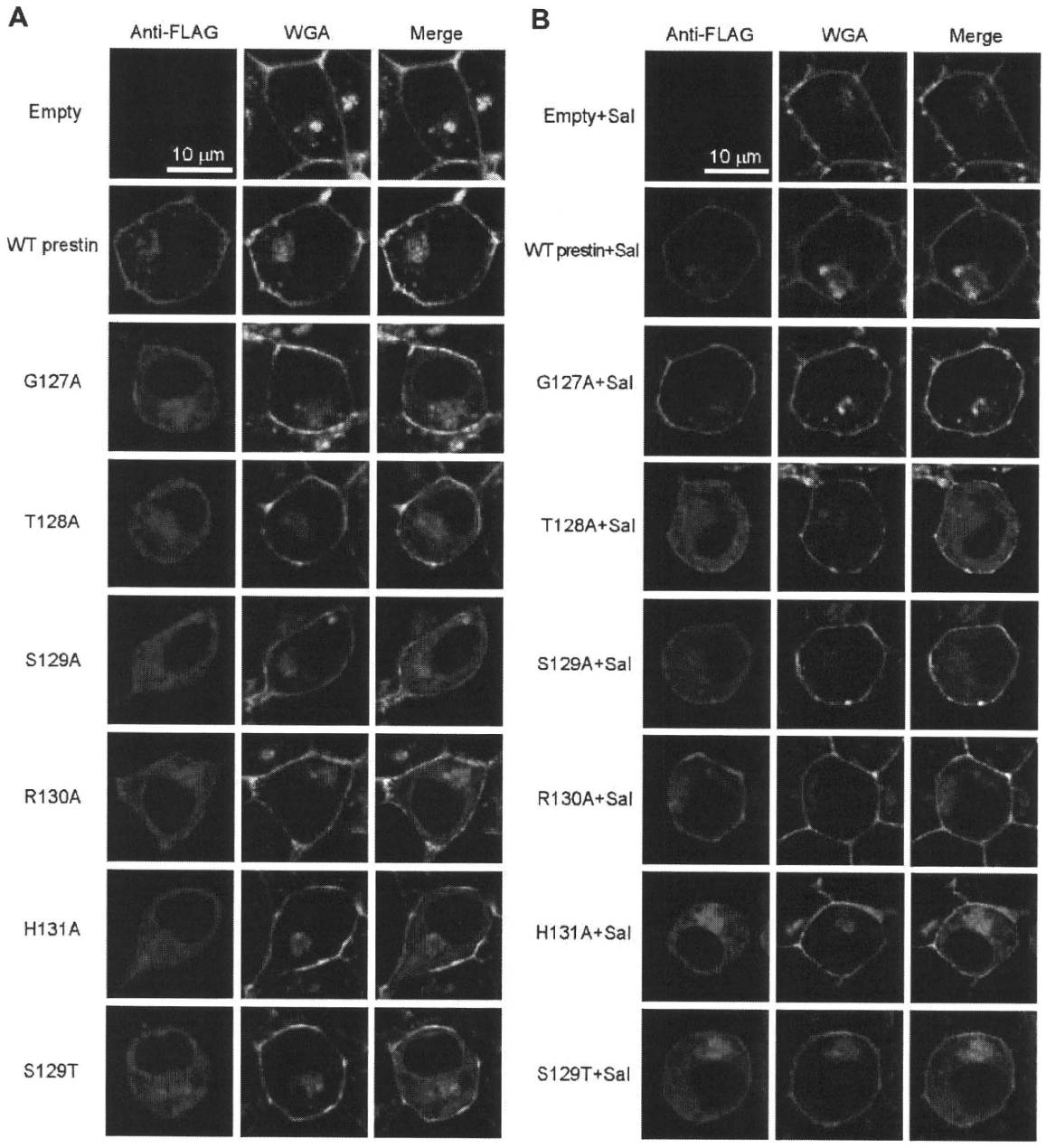

Fig. 1. Representative immunofluorescence images of transfected cells. (A) Stained cells cultured without 10 mM salicylate. (B) Stained cells cultured with 10 mM salicylate. Red and green fluorescence show prestin and both the plasma membrane and Golgi bodies, respectively. In the merged images, yellow–orange fluorescence indicates the co-localization of prestin and the plasma membrane, and that of prestin and the Golgi bodies.

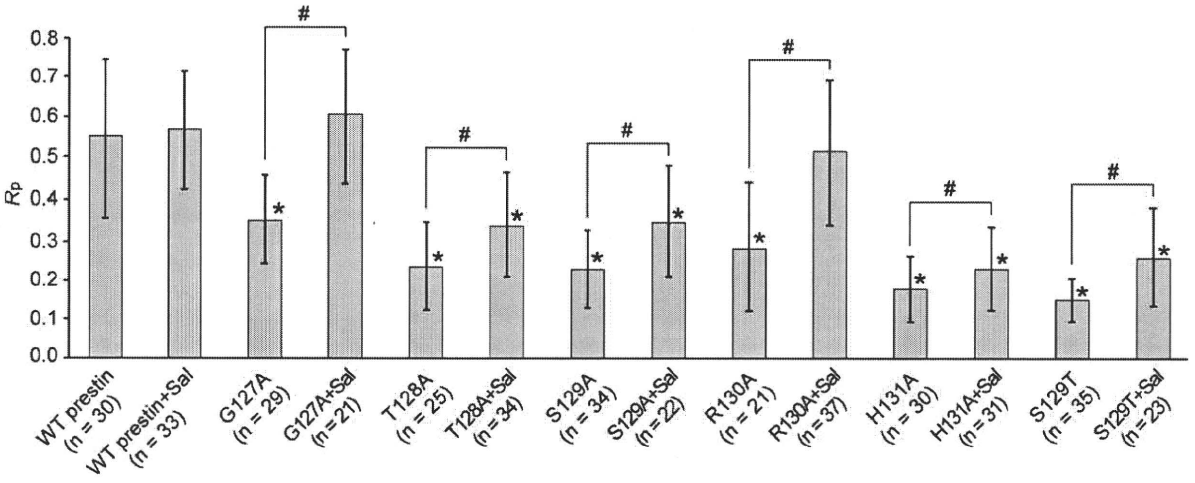

Fig. 2. R_p of WT prestin and its mutants. The R_p values of all prestin mutants were statistically lower than that of WT prestin when salicylate was not used, but they were increased by 10 mM salicylate. Asterisks show the statistical differences in the R_p values between WT prestin and the prestin mutants and between WT prestin+Sal and the prestin mutants+Sal ($p < 0.05$). Number signs indicate statistical differences between R_p values obtained from cells cultured with salicylate and those obtained from cells cultured without it in each prestin mutant ($p < 0.05$). Error bars show standard deviations.

each prestin mutant and the ratio of the amount of prestin in the plasma membrane to the total amount of prestin in the cell, R_p, was investigated. R_p was calculated by the following equation:

$$R_p = \frac{I_p}{I_w}, \tag{1}$$

where I_w is the sum of the intensity values of TRITC fluorescence of the whole area of the target cell which reflects the total amount of prestin in the cell, and I_p is the sum of the intensity values of TRITC fluorescence of only the pixels corresponding to the plasma membrane, which reflects the amount of prestin there. The I_w and I_p were calculated as described in our previous study [12].

2.4. Evaluation of electrophysiological properties of prestin

NLC, which is generally used for the analysis of prestin activity, was measured in the whole-cell patch-clamp recording as described in our previous study [13]. Transfected cells were washed just before the recording. By such washing, salicylate bound to prestin in the plasma membrane was expected to be dissociated [9]. The cells without membrane disruption which showed robust GFP fluorescence were selected for measurement. The recorded membrane capacitance was fitted with the first derivative of the Boltzmann function [14],

$$C_m(V) = C_{lin} + \frac{Q_{max}}{\alpha e^{\frac{V-V_{1/2}}{\alpha}}\left(1+e^{-\frac{V-V_{1/2}}{\alpha}}\right)^2}, \tag{2}$$

where C_{lin} is the linear capacitance, which is proportional to the membrane area of the cells, Q_{max} is the maximum charge transfer, V is the membrane potential and $V_{1/2}$ is the voltage at half-maximal charge transfer. In Eq. (2), α is the slope factor of the voltage-dependent charge transfer and is given by

$$\alpha = kT/ze, \tag{3}$$

where k is Boltzmann's constant, T is absolute temperature, z is valence and e is electron charge. To evaluate the maximum charge transfer of prestin in the unit plasma membrane, Q_{max}, which means the maximum charge transfer of prestin in whole plasma membrane, was divided by C_{lin} and designated as charge density.

For the comparison of NLC curve, NLC had to be normalized by the area of the plasma membrane. The normalized NLC $C_{nonlin/lin}$ was defined as

$$C_{nonlin/lin}(V) = \frac{C_{nonlin}}{C_{lin}} = \frac{(C_m(V) - C_{lin})}{C_{lin}}, \tag{4}$$

where C_{nonlin} is the nonlinear component of the measured membrane capacitance.

2.5. Concentration dependence of effects of salicylate on prestin

The relationship between the concentration of salicylate and the degree of the promotion of the plasma membrane expression of prestin mutants was investigated. The cells transfected with R130A were cultured with sodium salicylate at concentrations of 1 mM and 5 mM from 12 h after transfection. By the above-mentioned method, after 24 h of incubation, the cells were subjected to immunofluorescence staining and the R_p was then calculated.

3. Results and discussion

3.1. Localization of prestin in transfected cells

Representative immunofluorescence images of stained cells which were cultured without and with 10 mM salicylate are shown in Fig. 1A and B, respectively. To statistically investigate the localization of prestin in the cells, the R_p was calculated and shown in Fig. 2. Without salicylate, the R_p values of the prestin mutants were statistically lower than that of WT prestin ($p < 0.05$), suggesting that those mutants were accumulated in the cytoplasm. To confirm whether or not salicylate has the ability to promote the plasma membrane expression of the prestin mutants, prestin-transfected cells were cultured with 10 mM salicylate. The R_p of WT prestin was unchanged by 10 mM salicylate, indicating that such amount of salicylate did not affect the process of transport of WT prestin to the plasma membrane (Fig. 2). On the other hand, the R_p values of all prestin mutants statistically increased, compared with those when salicylate was not used ($p < 0.05$). Especially, the R_p of G127A+Sal and that of R130A+Sal were similar to that of WT prestin+Sal. These results indicate that salicylate promoted the plasma membrane expression of the prestin mutants accumulated in the cytoplasm.

3.2. Electrophysiological properties of prestin

The $C_{nonlin/lin}$ (V), and charge density and α of WT prestin and its mutants are shown in Figs. 3 and 4, respectively. Without

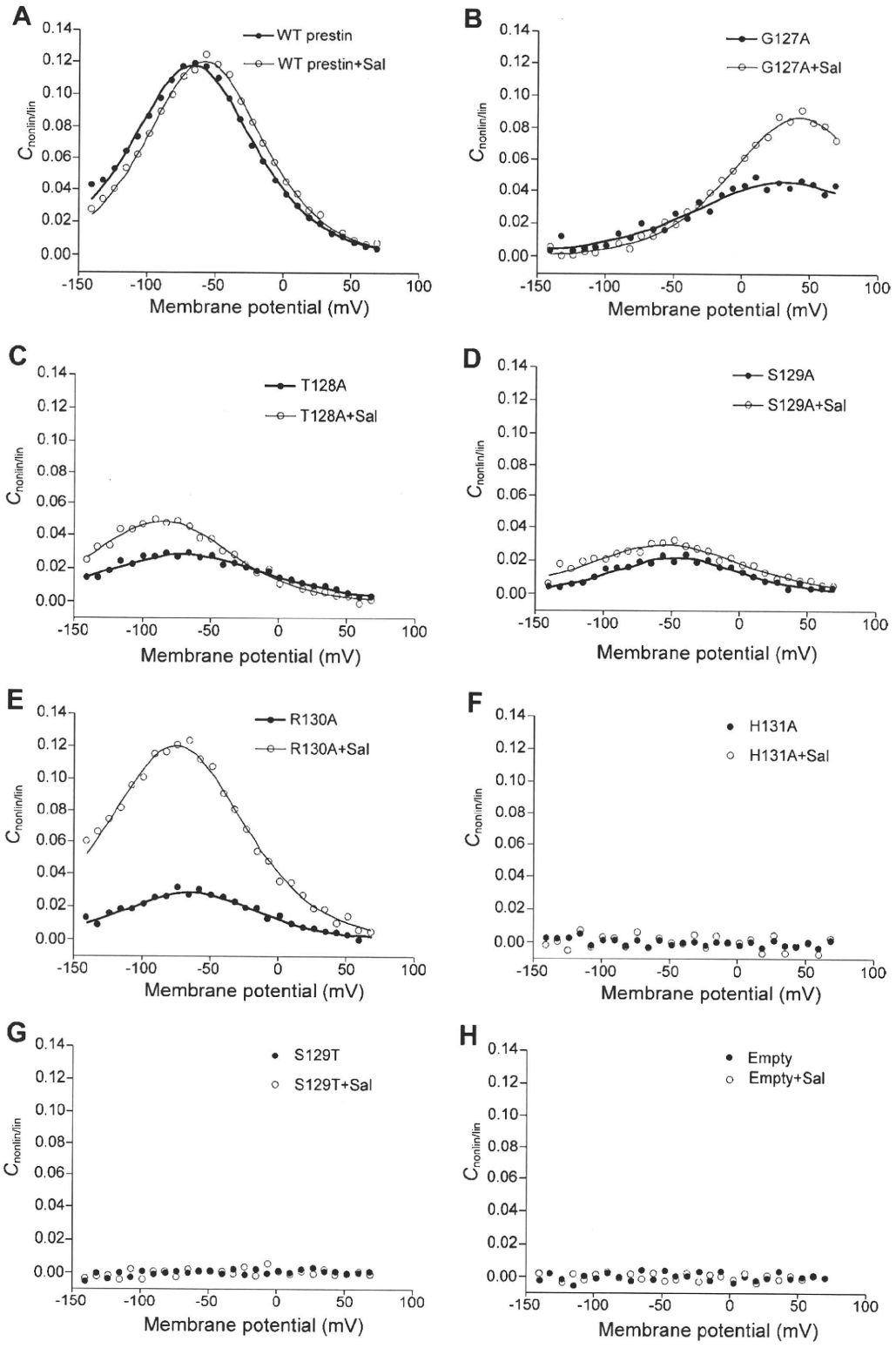

Fig. 3. Effects of salicylate on $C_{nonlin/lin}$ of prestin. Filled circles and thick lines show the results of transfected cells cultured without salicylate, while open circles and thin lines indicate the results of transfected cells cultured with 10 mM salicylate. (A) WT prestin and WT prestin+Sal. (B) G127A and G127A+Sal. (C) T128A and T128A+Sal. (D) S129A and S129A+Sal. (E) R130A and R130A+Sal. (F) H131A and H131A+Sal. (G) S129T and S129T+Sal. (H) Empty and Empty+Sal. When salicylate was used, NLC of G127A, T128A, S129A or R130A increased. On the other hand, in the case of H131A and S129T, NLC could not be detected in either type of cell, namely, cells cultured with and without 10 mM salicylate.

salicylate, G127A, T128A, S129A and R130A exhibited NLC, although their charge density was statistically smaller than that of WT prestin. On the other hand, H131A and S129T did not show NLC. The charge density of WT prestin+Sal was similar to that of WT prestin, suggesting that salicylate did not affect WT prestin itself nor the properties of the cells involved in the function of

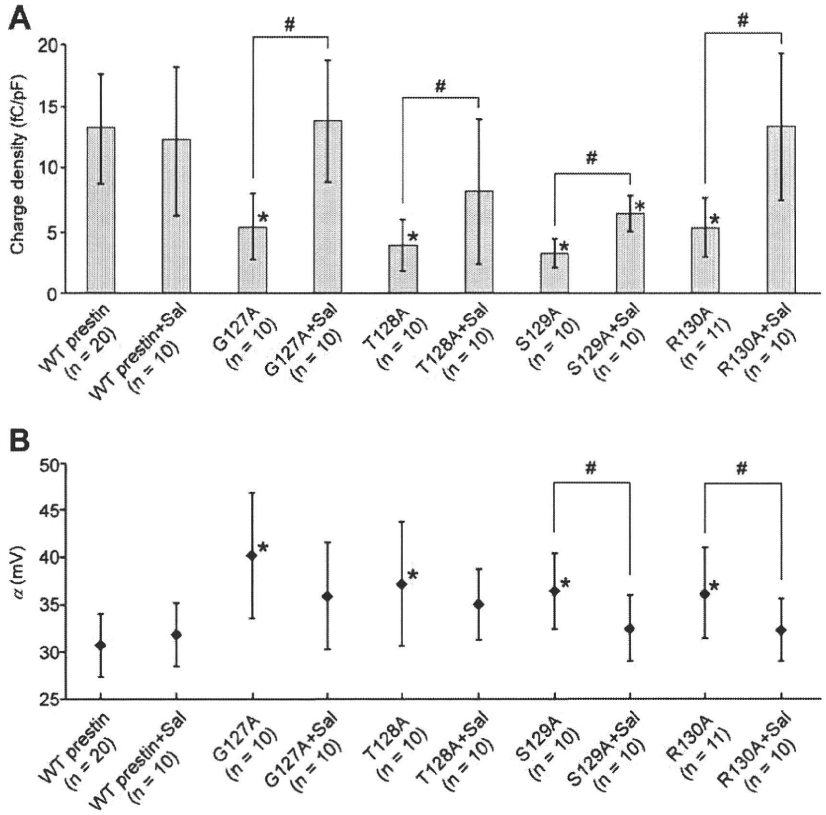

Fig. 4. Changes in the charge density and α of prestin by salicylate. (A) Charge density. The charge density of WT prestin was not affected by salicylate. On the other hand, the charge densities of G127A+Sal, T128A+Sal, S129A+Sal and R130A+Sal were statistically larger than those of G127A, T128A, S129A and R130A, respectively. (B) α. Without salicylate, the α values of G127A, T128A, S129A and R130A were statistically different from that of WT prestin. On the other hand, when 10 mM salicylate was used, there was no statistical difference in the α between the prestin mutants and WT prestin. Asterisks show the statistical differences in the charge density and α between WT prestin and the prestin mutants and between WT prestin+Sal and the prestin mutants+Sal ($p < 0.05$). Number signs indicate statistical differences in the charge density and α between cells cultured with salicylate and those cultured without it in each prestin mutant ($p < 0.05$). Error bars represent standard deviations.

prestin. On the other hand, the charge densities of G127A+Sal, T128A+Sal, S129A+Sal and R130A+Sal were statistically larger than those of G127A, T128A, S129A and R130A, respectively ($p < 0.05$). Especially, the charge density of G127A+Sal and that of R130A+Sal were similar to that of WT prestin+Sal. These results indicate that the charge density of those four mutants was recovered due to salicylate. On the other hand, H131A and S129T did not show NLC even when transfected cells were cultured with 10 mM salicylate.

The α was considered to represent properties of the anion binding of prestin [15]. Such values of G127A, T128A, S129A and R130A were statistically different from that of WT prestin when salicylate was not used (Fig. 4). On the other hand, when transfected cells were cultured with 10 mM salicylate, there was no statistical difference in α between the prestin mutants and WT prestin (Fig. 4). These results may imply that culturing the cells with salicylate somehow affects the properties of the anion binding of prestin.

3.3. Correlation between the R_p and the charge density

Without salicylate, the R_p values of all prestin mutants were lower than that of WT prestin. In this condition, the charge density of the prestin mutants was also lower or not recorded. On the other hand, salicylate increased both R_p and the charge density of G127A, T128A, S129A and R130A. Especially in G127A and R130A, R_p as well as the charge density recovered to the WT prestin level. This trend suggests that the changes in the charge density were correlated with changes in the R_P. Although R_p increased to some degree due to the addition of salicylate, H131A and S129T did not show NLC, possibly indicating that the amount of those mutants in the plasma membrane was still insufficient for detection of NLC. Another possibility is that H131A and S129T were promoted to be expressed in the plasma membrane but were non-functional.

Regarding S129A and S129T, the replacement of Ser-129 by threonine affected both the R_p and the charge density of prestin more strongly than that by alanine. Alanine and threonine are, respectively, smaller and larger than serine. Thus, the existence of an amino acid larger than serine at position 129 of prestin may be a steric constraint, affecting its characteristics significantly.

3.4. Changes in the concentration of salicylate

Salicylate at the concentration of 10 mM was found to recover the plasma membrane expression and the charge density of G127A and R130A to the WT prestin level as described above. Effects of decreasing the concentration of salicylate from 10 mM to 5 mM and 1 mM on the promotion of the plasma membrane expression were then evaluated using the cells transfected with R130A. Confocal images of the stained cells and calculated R_p are shown in Fig. 5A and B, respectively. The R_p of R130A was unchanged by 1 mM salicylate, while it was increased by 5 mM salicylate but not to the WT prestin level, suggesting that the promotion by salicylate of the plasma membrane expression of prestin mutants was concentration-dependent.

3.5. Discovery of new effect of salicylate on prestin

Salicylate is generally known to be an antagonist of prestin [8,9]. In the present study, another feature of salicylate was

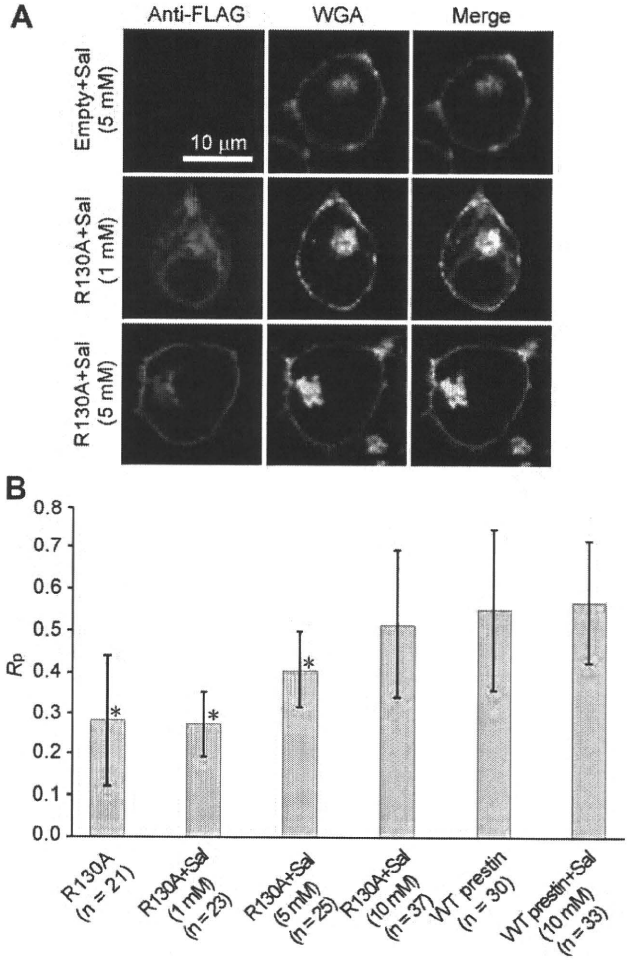

Fig. 5. Concentration dependence of the effects of salicylate on the localization of prestin. (A) Confocal microscopy images of stained cells. (B) Difference in the R_p due to the difference in the concentration of salicylate. The samples of R130A-expressing cells cultured without salicylate, with 1 mM salicylate, with 5 mM salicylate and with 10 mM salicylate are termed R130A, R130A+Sal (1 mM), R130A+Sal (5 mM) and R130A+Sal (10 mM), respectively, in this figure. In addition, the samples of WT prestin-expressing cells cultured without salicylate and with 10 mM salicylate are termed WT prestin and WT prestin+Sal (10 mM), respectively. The R_p of R130A was unchanged by 1 mM salicylate, but was increased by 5 mM salicylate. When transfected cells were cultured with 10 mM salicylate, the R_p recovered to the WT prestin level. Asterisks represent significance vs. WT prestin+Sal (10 mM) ($p < 0.05$). Error bars indicate standard deviations.

discovered, namely, it can promote the plasma membrane expression of prestin mutants accumulated in the cytoplasm, resulting in the recovery of the charge density. Various research findings have reported that if membrane proteins were accumulated in the cytoplasm due to their misfolding, a pharmacological chaperone bound to these proteins and then promoted their correct folding, resulting in their plasma membrane expression [3–7]. These reports may lead to a speculation that the prestin mutants analyzed in the present study were misfolded in the cytoplasm and that salicylate bound to these mutants and then induced their correct folding, promoting their transport to the plasma membrane. The next step of our study is to clarify if such speculation is correct, namely, to investigate the mechanism underlying the salicylate-induced recovery of the plasma membrane expression of prestin mutants.

Acknowledgements

This work was supported by Grant-in-Aid for Scientific Research on Priority Areas 15086202 from the Ministry of Education, Culture, Sports, Science and Technology of Japan, by Grant-in-Aid for Scientific Research (B) 18390455 from the Japan Society for the Promotion of Science, by Grant-in-Aid for Exploratory Research 18659495 from the Ministry of Education, Culture, Sports, Science and Technology of Japan, by a grant from the Human Frontier Science Program, by a Health and Labour Science Research Grant from the Ministry of Health, Labour and Welfare of Japan, and by Tohoku University Global COE Program "Global Nano-Biomedical Engineering Education and Research Network Centre" to H.W., and by a Grant-in-Aid for JSPS Fellows from the Japan Society for the Promotion of Science to S.K.

References

[1] Zheng, J., Shen, W., He, D.Z.Z., Long, K.B., Madison, L.D. and Dallos, P. (2000) Prestin is the motor protein of cochlear outer hair cells. Nature 405, 149–155.
[2] Ashmore, J. (2008) Cochlear outer hair cell. Physiol. Rev. 88, 173–210.
[3] Loo, T.W. and Clarke, D.M. (1997) Correction of defective protein kinesis of human P-glycoprotein mutants by substrates and modulators. J. Biol. Chem. 272 (2), 709–712.
[4] Loo, T.W., Bartlett, M.C. and Clarke, D.M. (2005) Rescue of folding defects in ABC transporters using pharmacological chaperones. J. Bioenerg. Biomembr. 37 (6), 501–507.
[5] Janovick, J.A., Maya Nunez, G. and Conn, P.M. (2002) Rescue of hypogonadotropic hypogonadism-causing and manufactured GnRH receptor mutants by a specific protein-folding template: misrouted proteins as a novel disease etiology and therapeutic target. J. Clin. Endocrinol. Metab. 87 (7), 3255–3262.
[6] Morello, J.P., Salahpour, A., Laperriere, A., Bernier, V., Arthus, M.F., Lonergan, M., Petaja Repo, U., Angers, S., Morin, D., Bichet, D.G. and Bouvier, M. (2000) Pharmacological chaperones rescue cell-surface expression and function of misfolded V2 vasopressin receptor mutants. J. Clin. Invest. 105 (7), 887–895.
[7] Ulloa-Aguirre, A., Janovick, J.A., Brothers, S.P. and Conn, P.M. (2004) Pharmacologic rescue of conformationally-defective proteins: implications for the treatment of human disease. Traffic 5 (11), 821–837.
[8] Tunstall, M.J., Gale, J.E. and Ashmore, J.F. (1995) Action of salicylate on membrane capacitance of outer hair cells from the guinea-pig cochlea. J. Physiol. 485, 739–752.
[9] Kakehata, S. and Santos-Sacchi, J. (1996) Effects of salicylate and lanthanides on outer hair cell motility and associated gating charge. J. Neurosci. 16 (16), 4881–4889.
[10] Kumano, S., Iida, K., Murakoshi, M., Naito, N., Tsumoto, K., Ikeda, K., Kumagai, I., Kobayashi, T. and Wada, H. (2005) Effects of mutation in the conserved GTSRH sequence of the motor protein prestin on its characteristics. JSME Int. J. 48C, 403–410.
[11] Kumano, S., Tan, X., He, D.Z.Z., Iida, K., Murakoshi, M. and Wada, H. (2009) Mutation-induced reinforcement of prestin-expressing cells. Biochem. Biophys. Res. Commun. 389, 569–574.
[12] Naoghare, P.K., Kwon, H.T. and Song, J.M. (2007) An automated method for in vitro anticancer drug efficacy monitoring based on cell viability measurement using a portable photodiode array chip. Lab Chip 7, 1202–1205.
[13] Iida, K., Tsumoto, K., Ikeda, K., Kumagai, I., Kobayashi, T. and Wada, H. (2005) Construction of an expression system for the motor protein prestin in Chinese hamster ovary cells. Hear. Res. 205 (1–2), 262–270.
[14] Santos Sacchi, J. (1991) Reversible inhibition of voltage-dependent outer hair cell motility and capacitance. J. Neurosci. 11, 3096–3110.
[15] Oliver, D., He, D.Z.Z., Klöcker, N., Ludwig, J., Schulte, U., Waldegger, S., Ruppersberg, J.P., Dallos, P. and Fakler, B. (2001) Intracellular anions as the voltage sensor of prestin, the outer hair cell motor protein. Science 292 (5525), 2340–2343.